Proceedings of the 8th International Conference of Control Systems, and Robotics (CDSR'21)
~~Niagara Falls, Canada~~ Virtual Conference– May 23-25, 2021
Paper No. 302
DOI: 10.11159/cdsr21.302

Kalman-filter-based Accurate Trajectory Tracking and Fault-Tolerant Control of Quadrotor

Rajamani Doraiswami[1], Lahouari Cheded[2], Marius Brinkmann[3]
[1]Department of Electrical and Computer EngineeringThe University of New Brunswick
Fredericton, NB, Canada, dorai@unb.ca
[2]Professor. Independent Researcher and Consultant, Life Senior MIEEE. UK cheded@kfupm.edu.sa
[3]Graduate student, Florida Polytechnic University
Fulbright scholar from Germany Brinkmann@floridapoly.edu

Abstract **-** A Kalman filter(KF)-based feedforward-feedback controller is proposed using the internal model(IM)-principle for accurate tracking of a desired trajectory, and fault-tolerant control of a quadrotor, despite input and output sensor measurements being affected by unknown disturbances, measurement noise and model perturbations. The quadrotor model is unstable and nonlinear. Its input is a nonlinear function of the roll, pitch and yaw, and its output is its position in the ground-fixed coordinates. The quadrotor is subject to model uncertainties, disturbances including wind gusts, aerodynamic drags, gravitational load, and Coriolis forces, and the inputs and the outputs are affected by unknown stochastic disturbances and measurement noise. Predictive analytics is used to estimate the true input by exploiting its smoothness and the randomness of the noisy input. The nonlinear system is better approximated using the linear parameter-varying (LPV) model described by piecewise-linear Box-Jenkins model at each operating point, than by conventional approximation techniques. The system and the associated Kalman filter (KF) are identified using novel emulator-generated data by minimizing the KF residual so that identified models are accurate, consistent and reliable. The proposed tracking, fault-tolerant control, and design of the KF residuals-based design of soft sensor were successfully evaluated on a simulated laboratory-scale quadrotor.

Keywords: nonlinear system, Box-Jenkins model, Kalman filter, linear parameter varying model, internal model principle.

1. Introduction

1.1 Problem Background

In recent years, autonomous systems are becoming increasingly important in academia, the industries, the military, and research funding agencies and are driven by exciting applications in the ground, air, and water vehicles, as well as in robotics. Model-based and model-free approaches including machine learning and artificial intelligence are employed in both terrestrial and aerial autonomous vehicles. To ensure autonomy, the controllers are designed to be highly adaptable to change and accommodate failures thanks to failure diagnosis, control reconfiguration, planning, and learning in addition to the conventional control functions such as tracking and regulation [1]. A feedback control system may be considered autonomous regarding stability goals concerning model uncertainties. This is because stability is maintained even in the face of parameter variations. This robustness is due to the embedded closed- loop mechanism that compensates for uncertainties.

Nonlinear model: The autonomous aerial vehicle (UAV), namely quadrotor is a second-order nonlinear system relating the position the vector of the center of mass of the quadrotor relative to the earth-fixed frame is described in the Cartesian coordinate system $\xi = (x, y, z) \in R^3$, and its orientation is expressed in Euler angle $\eta = (\phi, \theta, \psi) \in R^3$, namely the roll ϕ about the x axis, pitch θ about y and the yaw ψ about z [2-3]. There are four control inputs namely the torques implementing for the rotational motions ϕ, θ, ψ and the force f_{th} that drives the quadrotor. These quadrotors are subject several disturbances such as wind gusts, updrafts, aerodynamic drags, gravitational load, Coriolis, and centripetal forces. They fly at different altitudes and are subject to varying wind gusts that may cause accelerations or decelerations. As a result, the quadrotor is pushed away from the desired trajectory. Autonomous flight of quadrotor needs precise position and attitude information for control and stabilization. It carries sensors for measuring positions and orientations. The sensor measurements are corrupted by unknown stochastic disturbance and measurements noise. As a result, the output and the input are corrupted by the unknown disturbance and the measurement noise, and the model is an errors-in-variable one [4-5].

1.2 Main Contributions of This Paper

The key contributions of our study are briefly described below:

(a) ***Predictive analytics****:* Predictive analytics which is a deep learning algorithm is employed to estimate the true input from the corrupted input [6-7]. The resulting system model is described by a Box-Jenkins model that relates estimated true input and the corrupted output as explained next.

(b) ***Piecewise linear Box-Jenkins model*****:** As the analysis, design, estimation, identification, and control of a nonlinear system are not mathematically intractable; a linear parameter-varying (LPV) model is used to approximate the nonlinear system [8-12]. Its output is a sum of the signal (true output), the unknown stochastic, disturbance and measurement noise.

(c) ***System identification***: The static and dynamic behavior of the physical systems change as a result of variations of the parameters of the subsystems. The new ***emulators, used as a novel feature in this study, which are*** all-pass filters are connected to the accessible inputs and outputs in cascade with the subsystems during the offline system identification phase to mimic these model perturbations. The emulator-generated data covers both normal and abnormal operating scenarios including various types of faults (some totally unseen by the system as they are mimicked), and is employed in the identification of the system and the associated KFs [11-14]. The robust identification of the system and the associated Kalman filter is based on minimizing the Kalman filter residual and not the equation error since identified models are accurate *if and only if* Kalman filter residual is a zero-mean white noise process [13-15]. Further, it will ensure not only that the system model is accurately identified but also that the Kalman gain is optimal, thereby avoiding the need to specify the covariance of the disturbance and the measurement noise and the use of the Riccati equation to solve for the Kalman gain

*(d****) Novel use of Kalman filter***: The KF associated with the system plays a crucial role in the system identification, fault detection and isolation, and estimation of the signal, the output error (sum of the disturbance and measurement noise), signal and disturbance model in view of its key properties [11-15].

(e) ***Combined State Feedback -Feedforward controller:*** In order to track accurately the desired trajectory an *internal model principle* is used to design a feedback controller which is both necessary and sufficient for accurate tracking of an arbitrary waveform [16]. The feedforward controller is designed to track the desired reference feeding forward the reference signal. It is pro-active thanks to its predictive nature. It overcomes sluggish dynamics and delays without compromising the stability of the system. A combination of feedback and feedforward controllers can improve the performance significantly compared to using merely a feedback controller [17].

(f) ***Status monitoring, and fault tolerance:*** The two KFs, one associated with the system and the other with the signal model, are employed to develop a fault-tolerant, condition-based maintenance system, and a disturbance-tolerant (or disturbance-accommodating) system [13].

2. Modelling and Feedforward-Feedback Controller Design

We shall now give the key technical aspects of some of our main contributions, starting with the state-space modelling aspects of the quadrotors used.

2.1 State-Space Model of the Quadrotor

The state-space model is developed using the translational and rotational dynamics [2-3]:

$$\begin{aligned} \dot{\boldsymbol{x}} &= \boldsymbol{f}\left(\boldsymbol{x},\boldsymbol{u}\right); \boldsymbol{u} = \boldsymbol{g}_u\left(\boldsymbol{u}_0,\boldsymbol{d}_\eta,\boldsymbol{v}_\eta\right) \\ \boldsymbol{y} &= \boldsymbol{g}_y\left(\boldsymbol{x},\boldsymbol{d}_\xi,\boldsymbol{v}_\xi\right) \end{aligned} \tag{1}$$

Where $\boldsymbol{x} = \begin{bmatrix} \phi & \theta & \psi & \omega_\phi & \omega_\theta & \omega_\psi & \upsilon_x & \upsilon_y & \upsilon_z & x & y & z \end{bmatrix} \in R^{12}$; $\boldsymbol{u} \in R^4$ is an accessible corrupted input, ω_ϕ, ω_ϕ , ω_θ , and ω_ψ angular velocity about ϕ, θ, ψ , υ_x, υ_y, υ_z are linear velocity along x , y and z ; $\boldsymbol{u}_0 = \left(f_{th},\tau_\phi,\tau_\theta,\tau_\psi\right) \in R^4$ is true input, $\boldsymbol{d}_\eta \in R^4$ is the unknown stochastic disturbance, $\boldsymbol{v}_\eta \in R^4$ is the zero-mean white measurement noise corrupting the input $\boldsymbol{u}$, $\boldsymbol{y}(k) \in R^q$ is a vector formed of all measured (accessible) outputs and is corrupted by unknown zero-mean stochastic disturbance $\boldsymbol{d}_\xi \in R^q$ and $\boldsymbol{v}_\xi \in R^q$ zero-mean white measurement noise, $\boldsymbol{f}(.) \in R^q$, $\boldsymbol{g}_u(.) \in R^4$ and $\boldsymbol{g}_y(.) \in R^q$ are nonlinear functions.

Remarks: There are 3 translations (x, y, z) along the coordinates x, y and z axes, and 3 rotational motions about each of the coordinate axes. Euler angles (ϕ, θ, ψ) and their time derivatives do not depend on translational dynamics of (x, y, z) whereas the translation dynamics $(\ddot{x}, \ddot{y}, \ddot{z})$ depend on the Euler angle (ϕ, θ, ψ) and not on their derivatives. There are four control inputs (ϕ, θ, ψ) and f_{th} that drives the quadrotor along three translational components along the x, y and z axes as shown in Fig. 1.

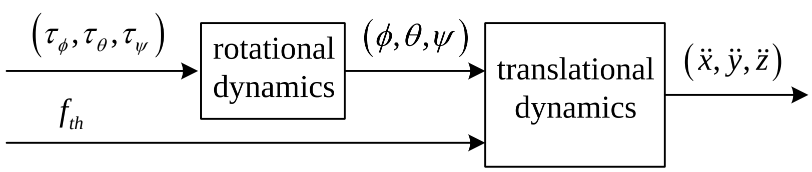

Fig. 1: Rotational and translation dynamics

2.2. Disturbance And Measurement Noise

Both the input $\boldsymbol{u}$ and the output $\boldsymbol{y}$ are corrupted by unknown stochastic disturbance and measurement noise. A model, whose input and output are both corrupted with noise, is termed as an errors-in variables model.

- The torque disturbance $\tau_w = (\tau_{w\phi}, \tau_{w\phi}, \tau_{w\psi}) \in R^3$ due to wind affects the angular velocity $\boldsymbol{\omega}_B = (\dot{\phi}_B, \dot{\theta}_B, \dot{\psi}_B)$
- The force disturbance $\boldsymbol{f}_{w\xi} = (f_{wx}, f_{wy}, f_{wz}) \in R^3$ due to wind affects the linear velocity $\boldsymbol{\upsilon}_B = (\upsilon_{Bx}, \upsilon_{By}, \upsilon_{Bz})$;

The torque rotation $\tau_w = (\tau_{w\phi}, \tau_{w\phi}, \tau_{w\psi})$ causes the quadrotor drone to tilt in varying directions depending on the direction and force of the wind. The force $\boldsymbol{f}_{w\xi} = (f_{wx}, f_{wy}, f_{wz}) \in R^3$ may accelerate or decelerate, push or pull the quadrotor. As a result of the presence of torque and force both caused by wind, the quadrotor trajectory is perturbed away from the desired trajectory.

Input disturbance: The zero-mean stochastic disturbance $\boldsymbol{d}_\eta(k)$ is modeled as the output of the state-space model $(\boldsymbol{A}_{d\eta}, \boldsymbol{B}_{d\eta}, \boldsymbol{C}_{d\eta})$ driven by a zero-mean white Gaussian noise process $\boldsymbol{u}_{d\eta}(k) \in R^3$, i.e.:

$$
\begin{aligned}
\boldsymbol{x}_{d\eta}(k+1) &= \boldsymbol{A}_{d\eta}\boldsymbol{x}_{d\eta}(k) + \boldsymbol{B}_{d\eta}\boldsymbol{u}_{d\eta}(k) \\
\boldsymbol{d}_\eta(k) &= \boldsymbol{C}_{d\eta}\boldsymbol{x}_{d\eta}(k) + \boldsymbol{v}_{d\eta}(k)
\end{aligned}
\tag{2}
$$

***Output disturbance*:** The output disturbance includes in addition to the zero-mean stochastic disturbance $(\boldsymbol{A}_{d\xi}, \boldsymbol{B}_{d\xi}, \boldsymbol{C}_{d\xi})$ driven by white Gaussian white noise process $\boldsymbol{u}_\xi(k) \in R^3$, and a deterministic $(\boldsymbol{A}_{dd\xi}, \boldsymbol{B}_{dd\xi}, \boldsymbol{C}_{dd\xi})$ driven by Kronecker Delta function denoted $\boldsymbol{\delta}(k) \in R^3$ .to mimic behavior the wind gusts.

.

$$
\begin{aligned}
\boldsymbol{x}_d(k+1) &= \boldsymbol{A}_d\boldsymbol{x}_d(k) + \boldsymbol{B}_d\boldsymbol{u}_d(k) \\
\boldsymbol{d}(k) &= \boldsymbol{C}_d\boldsymbol{x}_d(k) + \boldsymbol{v}_d(k)
\end{aligned}
\tag{3}
$$

Where $\boldsymbol{A}_d = \begin{bmatrix} \boldsymbol{A}_{d\xi} & 0 \\ 0 & \boldsymbol{A}_{dd\xi} \end{bmatrix} \in R^{n_d x n_d}$; $\boldsymbol{B}_d = \begin{bmatrix} \boldsymbol{B}_{d\xi} & 0 \\ 0 & \boldsymbol{B}_{dd\xi} \end{bmatrix} \in R^{n_d x 6}$; $\boldsymbol{u}_d(k) = \begin{bmatrix} \boldsymbol{u}_{\xi}(k) \\ \delta(k) \end{bmatrix} \in R^4$; $\boldsymbol{C}_d = \begin{bmatrix} \boldsymbol{C}_{d\xi} & \boldsymbol{C}_{dd\xi} \end{bmatrix} \in R^{3xn_d}$; $\boldsymbol{d}(k) = \boldsymbol{d}_{\xi}(k) + \boldsymbol{d}_{dd\xi}(k) \in R^3$

2.3 Predictive Analytics Approach

The inaccessible true input $\boldsymbol{u}_0(k)$ is buried in the input $\boldsymbol{u}(k)$ corrupted by the unknown stochastic disturbance $\boldsymbol{d}_{\eta}(k)$ and the measurement noise $\boldsymbol{v}_{\eta}(k)$. Exploiting the smoothness of $\boldsymbol{u}_0(k)$ and jaggedness of $\boldsymbol{d}_{\eta}(k)$ and $\boldsymbol{v}_{\eta}(k)$, the true input $\boldsymbol{u}_0(k)$ is estimated using predictive analytics approach [6-7]. The estimated input $\boldsymbol{u}_{est}$ then replaces the corrupted input $\boldsymbol{u}(t)$ in the rest of this paper.

2.4 Piecewise Linear Box-Jenkins Model and the Kalman Filter

A finite number of operating points are selected using scheduling variables for approximating the nonlinear system (1). Using the LPV approach, a piecewise linear Box-Jenkins (BJ) model and the associated KF are identified accurately using emulator-generated data at each operating point that approximates the nonlinear model (1) relating the estimated input $\boldsymbol{u}_{est}$ and the corrupted output $\boldsymbol{y}$.

Accurate Estimation: The signal $\boldsymbol{s}(k) \in R^{12}$ is the disturbance and measurement noise-free state of (1), the disturbance $\boldsymbol{\vartheta}_{\xi}(k) = \boldsymbol{d}_{\xi}(k) + \boldsymbol{v}_{\xi}(k)$, the disturbance and measurement noise-free model, termed signal model, $(\boldsymbol{A}_s, \boldsymbol{B}_s, \boldsymbol{C}_s)$ and the output disturbance model $(\boldsymbol{A}_d, \boldsymbol{B}_d, \boldsymbol{C}_d)$ are accurately estimated from the key properties of KF.

Box-Jenkins Model; An augmented model made of the signal model $(\boldsymbol{A}_s, \boldsymbol{B}_s, \boldsymbol{C}_s)$ and the output disturbance model $(\boldsymbol{A}_d, \boldsymbol{B}_d, \boldsymbol{C}_d)$ termed BJ becomes:

$$\begin{aligned} \boldsymbol{x}(k+1) &= \boldsymbol{A}\boldsymbol{x}(k) + \boldsymbol{B}\boldsymbol{u}_{sd}(k) \\ \boldsymbol{y}(k) &= \boldsymbol{C}\boldsymbol{x}_p(k) \end{aligned} \tag{4}$$

Where $\boldsymbol{x}(k) = \begin{bmatrix} \boldsymbol{x}_s(k) \\ \boldsymbol{x}_d(k) \end{bmatrix} \in R^n$; $\boldsymbol{A} = \begin{bmatrix} \boldsymbol{A}_s & 0 \\ 0 & \boldsymbol{A}_d \end{bmatrix} \in R^{nxn}$; $\boldsymbol{B} = \begin{bmatrix} \boldsymbol{B}_s & 0 \\ 0 & \boldsymbol{B}_d \end{bmatrix} \in R^{nx6}$; $\boldsymbol{C} = \begin{bmatrix} \boldsymbol{C}_s & \boldsymbol{C}_d \end{bmatrix} \in R^{6xn}$ $\boldsymbol{u}_{sd}(k) = \begin{bmatrix} \hat{\boldsymbol{u}}(k) & \boldsymbol{u}_d(k) \end{bmatrix}^T \in R^6$; $\boldsymbol{C}_p = \begin{bmatrix} \boldsymbol{C}_{rt} & \boldsymbol{C}_{tr} \end{bmatrix} \in R^{6xn}$; $n = 12 + n_d$

2.5 Feedback Controller: An Internal Model Approach

The desired trajectory, denoted $\boldsymbol{\xi}_d = (x_d, y_d, z_d) \in R^3$ is specified for the translation in the (x, y, z) plane. The four desired control inputs $(\phi_d, \theta_d, \psi_d)$ and f_{th} that drive the quadrotor along the three translational components x, y and z axes are computed using the inverse kinematics [2]

The objective is to design a feedback controller so that the closed-loop system formed of the signal model and the controller is asymptotically stable, its output tracks a given specified trajectory $\boldsymbol{\xi}_d = (x_d, y_d, z_d)$. It has been shown in [16] that the output of a linear time-invariant system will track a desired reference waveform despite the disturbance *if and only if* the controller includes internal models of the reference and the disturbance waveform driven by the error between the output and the desired reference waveforms.

Lemma:

Let $\boldsymbol{q}(k) \in R^3$ be the output of a signal model $(\boldsymbol{A}_s, \boldsymbol{B}_s, \boldsymbol{C}_s)$ and $\boldsymbol{q}_d(k)$ be the desired reference waveform. In the absence of disturbance, the robust asymptotic tracking holds:

$$\lim_{k \to \infty} it \{\boldsymbol{q}_d(k) - \boldsymbol{q}(k)\} = 0 \tag{5}$$

If and only if

- The state-space model of the signal model $(\boldsymbol{A}_s, \boldsymbol{B}_s, \boldsymbol{C}_s)$ is controllable and observable, i.e. there is no pole-zero cancellations in the plant transfer function.
- A model of the system that has generated the reference input $\boldsymbol{q}_d(k)$, termed as 'an internal model of reference ' , is included in the controller and the internal model $(\boldsymbol{A}_I, \boldsymbol{B}_I, \boldsymbol{C}_I)$ of the desired trajectory $\boldsymbol{q}_d(k)$ is driven by the tracking error $\boldsymbol{e}_{tr}(k) = \boldsymbol{q}_d(k) - \boldsymbol{q}(k)$
- $\begin{vmatrix} zI - \boldsymbol{A}_s & \boldsymbol{B}_s \\ \boldsymbol{C}_s & 0 \end{vmatrix} \neq 0$ for all $\{z : |z\boldsymbol{I} - \boldsymbol{A}_I| = 0\}$ That is, there are no pole-zero cancellations between the poles of the internal model and the zeros of the plant.
- The resulting closed-loop system formed of the controller and the plant is stabilized

The asymptotic tracking holds independent of all variations in the plant and in the stabilizer parameters as long as a) the closed-loop system is asymptotically stable, and b) the internal model parameters are not perturbed

Corollary**:** If the output is corrupted by a known deterministic disturbance, $\boldsymbol{y}(k) = \boldsymbol{s}(k) + \boldsymbol{y}_{dd}(k)$ where $\boldsymbol{y}_{dd}(k)$ is the output of a known deterministic and asymptotically-stable linear time-invariant system, then robust asymptotical tracking occurs

$$\lim_{k\to\infty} it \{\boldsymbol{q}_d(k) - \boldsymbol{q}(k)\} = 0 \tag{6}$$

If and only if the internal models of both the reference input and the known deterministic disturbance model are included in the controller.

Proof**:** the proof is given in [15]

A feedback controller is thus designed using the internal model principle to track the desired reference despite the perturbation in the system. The internal model $(\boldsymbol{A}_I, \boldsymbol{B}_I, \boldsymbol{C}_I)$ that generates the reference input $\boldsymbol{q}_d(k)$ is

$$\begin{aligned} \boldsymbol{x}_I(k+1) &= \boldsymbol{A}_I \boldsymbol{x}_I(k) + \boldsymbol{B}_I \boldsymbol{e}(k) \\ \boldsymbol{y}_I(k) &= \boldsymbol{C}_I \boldsymbol{x}_I(k) \end{aligned} \tag{7}$$

Where $\boldsymbol{A}_I \in R^{n_I x n_I}$ $\boldsymbol{B}_I \in R^{n_I x 6}$; $\boldsymbol{C}_I = \boldsymbol{I} \in R^{n_I x n_I}$ is an identity matrix; $\boldsymbol{e}(k) = \boldsymbol{q}_d(k) - \boldsymbol{y}(k) \in R^6$ is the error

Fig. 2 below shows the closed-loop signal model formed of the plant model, and the combined state-feedback and feedforward controller:

$$\begin{aligned} \boldsymbol{u}_p &= \boldsymbol{u}_{ff} - \boldsymbol{F}_I \boldsymbol{x}_I \\ \boldsymbol{u}_s &= \boldsymbol{u}_p - \boldsymbol{F}_s \boldsymbol{x}_s \end{aligned} \tag{8}$$

Where $\boldsymbol{x}_I$ is the state of the internal model $(\boldsymbol{A}_I, \boldsymbol{B}_I, \boldsymbol{C}_I)$; $\boldsymbol{u}_p$ is the input that drives the closed loop signal model; $\boldsymbol{F}_I$ and $\boldsymbol{F}_s$ are state feedback gains. The state-feedback controller $\boldsymbol{u}_{fb} = \boldsymbol{F}_s \boldsymbol{x}_s$ is an optimal linear quadratic regulator obtained from the parameterization of all stabilizing controllers to ensure robustness to model perturbations.

2.5.1 Feedforward Controller

The objective of the feedforward controller is to provide a unity transfer function from reference input $\boldsymbol{q}_d$ to the output $\boldsymbol{q}$ by choosing feedforward transfer function $\boldsymbol{H}_{ff}(z)$ such that:

$$\boldsymbol{G}_{cl}(z) \boldsymbol{H}_{ff}(z) = \boldsymbol{I} \tag{9}$$

Even in the presence of model perturbations, the feedforward controller can mitigate the effect of the output error on the performance of the combined controller. The feedforward controller rejects quickly the output error without waiting for the deviation in the output to occur, hence its anticipatory action. The reference input is injected into the feedforward path to reject the effects of the output error on the output, thereby ensuring that the output is generated by the reference input and not by the output error. The feedforward controller is given by:

$$\boldsymbol{u}_{ff}(z)=\boldsymbol{H}_{ff}\,\boldsymbol{q}_d(z) \tag{10}$$

The expression for $\boldsymbol{H}_{ff}\in R^{6x6}$ is given in the later section 4.3.1.

2.5.2 Closed-Loop Signal Model

The augmented closed loop model $(\boldsymbol{A}_{cl},\boldsymbol{B}_{cl},\boldsymbol{C}_{cl})$ shown in Fig. 2 is formed of the signal model $(\boldsymbol{A}_s,\boldsymbol{B}_s,\boldsymbol{C}_s)$, and the internal model $(\boldsymbol{A}_I,\boldsymbol{B}_I,\boldsymbol{C}_I)$ (7) of the desired reference $\boldsymbol{q}_d(k)$. Using the feedback controller (8) and feedforward controller (10) yields:

$$\begin{aligned}\boldsymbol{x}_{cl}(k+1)&=\boldsymbol{A}_{cl}\boldsymbol{x}_{cl}(k)+\boldsymbol{B}_{cl}\boldsymbol{q}_d(k)\\ \boldsymbol{q}(k)&=\boldsymbol{C}_{cl}\boldsymbol{x}_{cl}(k)\end{aligned} \tag{11}$$

Where $\boldsymbol{x}_{cl}(k)=\begin{bmatrix}\boldsymbol{x}_s\\ \boldsymbol{x}_I\end{bmatrix}\in R^{n_{cl}}$, $\boldsymbol{A}_{cl}=\begin{bmatrix}\boldsymbol{A}_s-\boldsymbol{B}_s\boldsymbol{F}_s & -\boldsymbol{B}_s\boldsymbol{F}_I\\ -\boldsymbol{B}_I\boldsymbol{C}_s & \boldsymbol{A}_I\end{bmatrix}\in R^{n_{cl}xn_{ci}}$, $\boldsymbol{B}_{cl}=\begin{bmatrix}\boldsymbol{B}_{cl}\boldsymbol{H}_{ff}\\ \boldsymbol{B}_I\end{bmatrix}\in R^{n_{cl}x6}$, $\boldsymbol{C}_{cl}=\begin{bmatrix}\boldsymbol{C}_I & \boldsymbol{C}_s\end{bmatrix}\in R^{6xn_{cl}}$

2.6 Combined Feedforward-Feedback Controller

The diagrammatic representation of the feedforward-feedback controller is depicted below in Fig. 2.

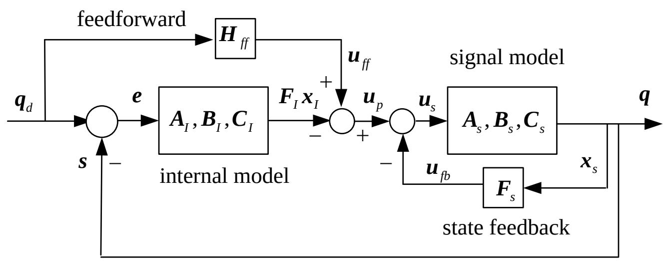

Fig. 2: Closed-loop signal model

2.7 Closed Loop Box-Jenkins Model

The Box-Jenkins model $(\boldsymbol{A},\boldsymbol{B},\boldsymbol{C})$ relating the corrupted output $\boldsymbol{y}(k)$ and the desired reference input $\boldsymbol{q}_d(k)$, termed system model, the augmented model formed of the internal model-based closed-loop control system $(\boldsymbol{A}_{cl},\boldsymbol{B}_{cl},\boldsymbol{C}_{cl})$ (11) and the combined stochastic disturbance model and the deterministic disturbance model (3) is given by:

$$\begin{aligned}\boldsymbol{x}(k+1)&=\boldsymbol{A}\boldsymbol{x}(k)+\boldsymbol{B}\boldsymbol{r}(k)\\ \boldsymbol{y}(k)&=\boldsymbol{C}\boldsymbol{x}(k)+\boldsymbol{v}(k)\end{aligned} \tag{12}$$

$$\boldsymbol{x}=\begin{bmatrix}\boldsymbol{x}_s\\ \boldsymbol{x}_{dr\xi}\\ \boldsymbol{x}_{dd\xi}\end{bmatrix}\in R^n;\ \boldsymbol{A}=\begin{bmatrix}\boldsymbol{A}_{cl} & -\boldsymbol{B}_{cl}\boldsymbol{C}_{dr\xi} & -\boldsymbol{B}_{cl}\boldsymbol{C}_{dd\xi}\\ 0 & \boldsymbol{A}_{dr\xi} & 0\\ 0 & 0 & \boldsymbol{A}_{dd\xi}\end{bmatrix}\in R^{nxn};\ \boldsymbol{B}=\begin{bmatrix}\boldsymbol{B}_{cl} & o & 0\\ 0 & \boldsymbol{B}_{d\xi} & 0\\ 0 & 0 & \boldsymbol{B}_{dd\xi}\end{bmatrix}\in R^{nx9};\ \boldsymbol{C}=\begin{bmatrix}\boldsymbol{C}_{cl} & \boldsymbol{C}_{d\xi}\end{bmatrix}\in R^{6xn};\ \boldsymbol{y}(k)\in R^q;$$

$$\boldsymbol{r}(k)=\begin{bmatrix}\boldsymbol{q}_d(k) & \boldsymbol{u}_\xi(k) & \delta(k)\end{bmatrix}^T\in R^9$$

3. Evaluation on Simulated Model of a Quagrotor

3.1 Predictive Analytics

The inaccessible signal $u_0(k)$ is extracted from the corrupted input $u(k)$ using the frequency-domain approach by exploiting their spectral characteristics such as the smooth waveform $u_0(k)$ has line-spectra, and noisy $\vartheta_u(k)$ has wildly-varying spectra. We assume that the true input is constant. Fig. 3 shows the true input u_0, estimated true input $\hat{u}$, the corrupted input u and their spectra. Subfigures A and B show the true input u_0 and its spectra using Fast Fourier Transform (FFT).Subfigures C and D show the FFT spectra spectrum of the signal u_{0i}, and the true signal.

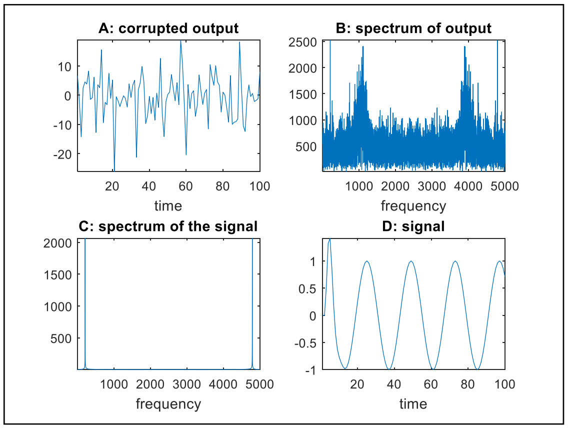

Fig. 3: Signal estimate from corrupted output

3.2 The Feedforward-Feedback Controller Scheme

The proposed feedforward-feedback controller scheme is evaluated on a simulated model of a drone moving in a horizontal plane to track accurately the desired trajectory despite wind gusts and model perturbations. The performance of the proposed controller is compared with that of the conventional combined controller. The input and the output of the quadrotor are both corrupted by exogenous and endogenous stochastic disturbance and measurement noise.

3.3 The Extraction of the Signal Using Kalman Filter

The proposed KF and the internal model-based combined state feedback and feedforward shown the block diagram of Fig. 2 is evaluated using Box-Jenkins model. The desired translation trajectory in $(x.y,z) \in \mathbb{R}^3$ is:

$$\left(x_d(k), y_d(k), z_d(k)\right) = \left(\cos\left(\pi k/12\right), \sin\left(\pi k/12\right), 1\right) \qquad (13)$$

Using the inverse kinematics, the desired control input $\left(\phi_d, \theta_d, \psi_d\right)$ is determined.

Fig. 4 (a, b) show the signals of interest, which are the desired outputs $\left(x_d, y_d, z_d\right)$, the desired Euler angles $\left(\phi_d, \theta_d, \psi_d\right)$, and the corresponding corrupted measurement outputs. Subfigures A, B and C of Fig 4 a: shows $\left(x_d, y_d, z_d\right)$, their Kalman; filter estimates and the outputs while Fig. 4 b shows $\left(\phi_d, \theta_d, \psi_d\right)$, their KF estimates and the outputs. The KF estimates of the signals are accurate and are devoid of any random fluctuations.

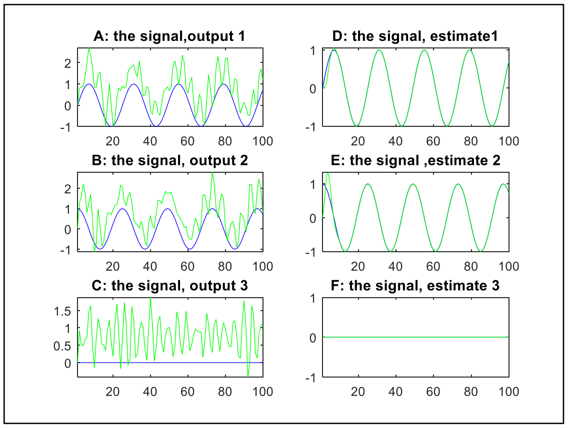

Fig. 4 a: Positions, outputs and estimates

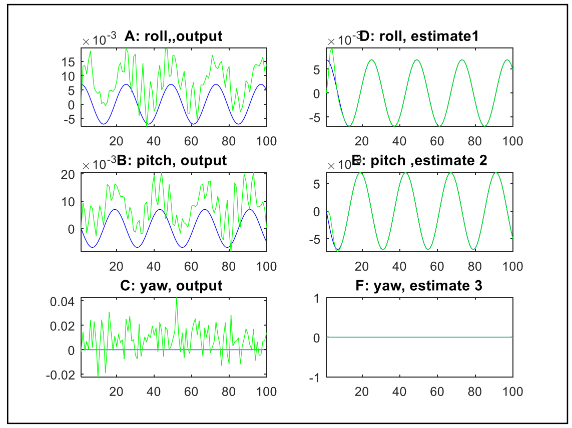

Fig. 4 b: Euler angles, outputs and estimates

Remarks**:** The internal model includes only the reference signal as the deterministic disturbance is unknown, and, by its very design, the internal model cannot handle stochastic waveforms [15]. Hence the combined effect of the unknown deterministic disturbance, stochastic disturbance and measurement noise, continues to be present in the output, which is exhibited respectively as an offset and random fluctuations in the outputs, as shown in subfigures A, B and C of Fig. 3 a and Fig. 3 b. The subfigures D, E, and F in these 2 figures show that the accurate KF estimates of the true signals from the corrupted outputs. It can be deduced that the objective of the quadrotor is to track accurately the desired circular trajectory in the (x, y) plane and remain stationary along the z-axis at a desired fixed position despite the presence of the disturbance and measurement noise corrupting the measurement output, thus amounting to an accurate trajectory tracking while hovering in a stable manner at a given altitude along the z-axis. The importance of estimating the true signal accurately despite disturbance such as wind gusts that may accelerate or decelerate, push or pull the quadrotor away from the desired trajectory is clearly emphasized here.

3.4 Tracking Performance: Comparison between Proposed and Conventional Controllers

Fig. 5 compares the tracking performances of the proposed and the conventional control schemes. Subfigure A shows the desired trajectory (x_d, y_d) . Subfigure B shows the performance of the proposed scheme where an internal model for the feedback controller, and the KF estimates, are both used but with no feedforward controller used. Subfigures C shows the trajectory when the internal model-based controller is used but without the help of any KF to provide the required accurate signal estimates. In this case, the output will remain corrupted by the deterministic and stochastic disturbances and the measurement noise. Subfigure D shows the proposed control scheme to track the desired trajectory that is based on the combined feedback-feedforward controller (in blue) and is compared with the ideal one (in red).

Thanks to the above-cited properties of the KF, and the help of the predictive power of the feedforward controller added at a small operational cost only, an accurate trajectory tracking has been achieved. Note here that the desired trajectory is shown in all subfigures as a reference and for ease of comparison between the different control schemes.

Important remark on extending this work: The trajectory tracking scheme described above can be readily extended to include any arbitrary smooth trajectory using various function approximation schemes. This extension work is currently underway.

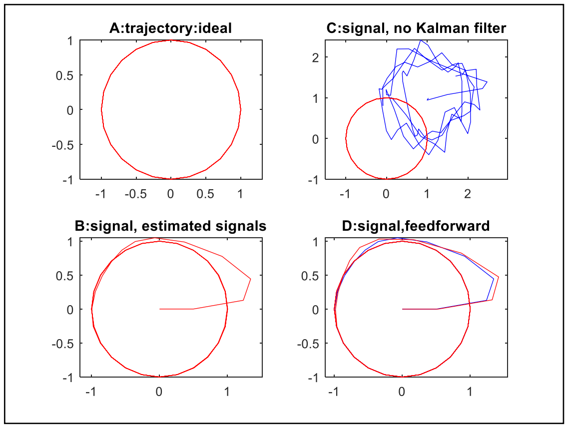

Fig. 5: Evaluation of the proposed controller

3.5 Status monitoring, Condition-Based Monitoring, Soft Sensing and Fault Tolerance

The residuals $\boldsymbol{e}_{kf}(k)$ of the system KF and $\boldsymbol{e}_{ks}(k)$ of the signal KF are employed to monitor the status of the overall system and to detect and isolate faults in the signal and disturbance models and the sensors. The proposed scheme provides a sound framework for developing fault-tolerant systems and condition-based maintenance systems as well. An efficient scheme to monitor the status of the system may be implemented. First the status of the system is monitored by analyzing the residual of the KF of the system model. If there is a variation, then the residual of the KF of the signal model is analyzed to ascertain whether a fault has occurred. Some key aspects of these by-product applications, which gave rise to the design of a novel soft sensor, are briefly discussed here as they will be reported elsewhere in greater details.

(a) ***Fault Isolation****:* If the performance degradation is high or the controller adaptation fails to meet the acceptable bound, the presence of a fault is then asserted. The faulty subsystem is then isolated using the influence vector defined in [12]. The faulty subsystem is either repaired or replaced.

(c) ***Fault tolerance****:* If there is performance degradation, then the controller is redesigned (adapted) or the plant re-identified, thereby "nipping the incipient faults in the bud" and preventing them from growing into serious faults capable of damaging the system, and possibly causing all the concomitant nefarious consequences, including system breakdown, loss of productivity and danger to the operating personnel. The role of the fault-tolerant system consists of effectively and reliably performing the following functions: a) condition monitoring, b) detection of performance degradation, c) controller adaptation, and d) detection and isolation of faults.

3.6 Kalman Filter-Based Fault Tolerance

The objective of a drone is to track accurately the desired trajectory despite wind gusts and model perturbations. The measure of performance is the KF residual. If the residual is a zero-mean white noise process, the tracking performance would be acceptable. Otherwise, the fault is identified and accommodated. The KF forms the backbone for developing the fault-tolerant system. In so doing, it monitors the system performance and accurately diagnoses faults (if any) thanks to the use of the powerful emulators.The KF residual monitors the condition of the system, detect the incipient fault and help isolate faulty subsystems, namely the actuator, plant, and the sensors. The non-whiteness of the KF residual is an indicator of an incipient fault while a zero-mean white noise residual indicates that the system is healthy. The autocorrelation of the residual gives a visual indication of the system health while the variance of the residual, which is the autocorrelation evaluated at the origin indicates the size of the incipient fault. Fig 6: shows the autocorrelations of the residual when there is an incipient fault in the actuator, sensor and the signal model. Subfigures A, B, and C show the autocorrelation of the residual when the actuator, the sensor and the plant are respectively perturbed. The autocorrelation is not a zero-mean white noise process as there are fault indicator terms in each of these 3 cases. Subfigure D shows that the autocorrelation is zero-mean white noise process implying that there are no perturbations and the system is structurally healthy.

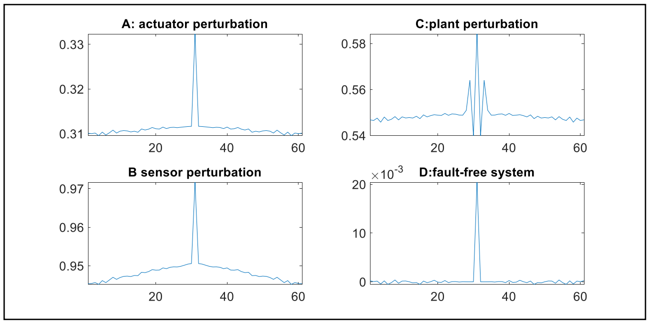

Fig 6 : Autocorrelation of the residual for faulty subsystems and a fault-free system

4. Conclusions

In this paper, a novel approach is proposed to accurately track the desired trajectory of a quadrotor, in the face of unknown deterministic and stochastic disturbances and measurement noise, and hence, without requiring their statistics as is done in conventional approaches. The proposed approach is based on the use of the powerful KF and the internal model principle to efficiently design a combined feedforward-feedback controller to accurately guide the quadrotor along the desired trajectory while combatting the undesirable and disturbing effects such as wind gusts. The internal model successfully tracks the desired reference as the internal model includes the modes of the reference model only but not those of the unknown disturbance model as it is not geared for such signals. The tracking error is noisy as it is subject to an offset due to deterministic disturbance. To overcome the inaccurate tracking, key properties of the KF were employed for estimating the deterministic disturbance, then the signal and signal model from the output corrupted by unknown disturbances and measurement noise. The models of the system, and the signal as well as their associated KFs, were also directly identified using only the residuals of these KF. As a by-product, a novel KF-based soft sensor has also been developed to replace the error- and maintenance-prone hardware sensor to estimate the required position and the rotations angles and their derivatives, in a differentiation-free manner. Thanks to the availability of the powerful KFs and the key properties of their residuals, and to the design of the novel soft sensor, a fault-tolerant has also been developed which ensures key functions such as monitoring of the system performance, detection, isolation and accommodation of the detected faults. Our approach also offers an efficient way of analyzing the KF’s residual by distinguishing between spurious and random variations in the disturbance model and a fault-indicative structural variation in the signal model. The presence of the latter term indicates reliably the presence of a fault and hence helps in ensuring a low false- alarm. The proposed scheme has been successfully evaluated on the simulated quadrotor. Work is currently underway to evaluate it on a physical quadrotor.

Acknowledgements

The first author acknowledges Mr. Mustapha Achoubane, the Associate Director of International Studies, Professor Muhammad Rashid od Florida Polytechnic, Lakeland, Florida, USA, faculties, and the graduate students, and the University of New Brunswick, Fredericton, New Brunswick, Canada

References

[1] Antsaklis, P, Editorial, Control Systems and the Quest for Autonomy IEEE transactions on automatic control, vol. 62, no. 3, March 2017

[2] Mohamed Fanni and Ahmed Khalifa, (2017),“A New 6-DOF Quadrotor Manipulation System: Design, Kinematics, Dynamics, and Control” IEEE/ASME Transactions On Mechatronics, VOL. 22, NO. 3, pp; 1315-1326

[3] Xiaodong Zhang, Xiaoli Li, Kang Wang, and Yanjun Lu,(2014),“A Survey of Modelling and Identification of Quadrotor Robot”, Hindawi Publishing Corporation, ID 320526, http://dx.doi.org/10.1155/2014/320526

[4] T.Soderstrom,(2006),“System Identification for the Errors in-Variables Problem”, Transactions of the Institute of Measurement and Control 34(7) 780–792

[5] Stephane Thil, et.,al., (2009), “Unifying some higher-order statistic-based methods for errors-in-variables model identification”, Automatica 45, 8, DOI:10.1016
[6] Guest Editorial: Emerging Trends in LPV-Based Control of Intelligent Automotive Systems, Vol. 14, Issue 18, 17 December 2020, IET Control Theory & Applications
[7] D. Abbott (2014), “Applied Predictive Analytics: Principles and Techniques for the Professional Data Analyst”, *John Wiley & Sons*
[8] G. J. Mallory and R. Doraiswami (1999), A Filter for On-line Estimation of Spectral Content, IEEE Transactions on Instrumentation and Measurement, Vol. 48, No.6, pp. 1047-1055
[9] Guest Editorial: Emerging Trends in LPV-Based Control of Intelligent Automotive Systems, Vol. 14, Issue 18, 17 December 2020, IET Control Theory & Applications
[10] T'oth, R, H Abbas, and W Werner (2011). "On the State Space Realization of LPV input-output model: practical approaches." IEEE Transactions on Control Systems Technology 20; No 1; pp: 139-153.
[11] Damiano Rotondo, (2017) Robust State-Feedback Control of Uncertain LPV SystemsAdvances in Gain-Scheduling and Fault Tolerant Control Techniques pp 75-99, Springer
[12] Doraiswami, R, and Cheded, L (2015). "Linear Parameter Varying Modelling and Identification for Condition-based Monitoring of Systems." *Journal of Franklin Institute* 352, no. 4 : 1766-1790
[13] Doraiswami, R, and Cheded, L (2015). "Linear Parameter Varying Modelling and Identification for Condition-based Monitoring of Systems." *Journal of Franklin Institute* 352, no. 4 : 1766-1790
[14] Doraiswami, R and Cheded. L. (2017), Robust Fault-Tolerant Control Using an Accurate Emulator-Based Identification Technique, International Journal of Contro*l*, ISSN: 0020-7179, 1336-5820
[15] R. Doraiswami and L. Cheded (2018), Robust Kalman Filter-Based Least Squares Identification of a Multi Variable System, IET Control Theory and Applications, The Institution of Engineering and Technology, ISSN 1751-8644, www.ietdl.org
[16] Doraiswami, R, C Diduch, and M Stevenson, (2014), Identification of Physical Systems: Applications to Condition Monitoring, Fault Diagnosis, Soft Sensor and Controller Design. John Wiley and Sons, ISBN 9781119990123
[17] Francis, Bruce, F, and Murry, Wonham, W, (1976) "The Internal Model Principle of Control Theory." *Automatica* 12: 457-465
[18] Seborg, D.E, T.F Edgar, and D.A Mellichamp. 2004. *Process Dynamics and Control: Second Edition.* NY: John Wiley and Sons